Author/s:
Zhou, W;Van Sinderen, M;Rainczuk, K;Menkhorst, E;Sorby, K;Osianlis, T;Pangestu, M;Santos, L;Rombauts, L;Rosello-Diez, A;Dimitriadis, E

Title:
Dysregulated miR-124-3p in endometrial epithelial cells reduces endometrial receptivity by altering polarity and adhesion

Date:
2024-10-08

Citation:
Zhou, W., Van Sinderen, M., Rainczuk, K., Menkhorst, E., Sorby, K., Osianlis, T., Pangestu, M., Santos, L., Rombauts, L., Rosello-Diez, A. & Dimitriadis, E. (2024). Dysregulated miR-124-3p in endometrial epithelial cells reduces endometrial receptivity by altering polarity and adhesion. Proceedings of the National Academy of Sciences of the United States of America, 121 (41), https://doi.org/10.1073/pnas.2401071121.

Persistent Link:
https://hdl.handle.net/11343/358809

PNAS RESEARCH ARTICLE | DEVELOPMENTAL BIOLOGY

Dysregulated miR-124-3p in endometrial epithelial cells reduces endometrial receptivity by altering polarity and adhesion

Wei Zhou[a,b,1], Michelle Van Sinderen[c,1], Katarzyna Rainczuk[c], Ellen Menkhorst[a,b,c], Kelli Sorby[c,d], Tiki Osianlis[e], Mulyoto Pangestu[e,f], Leilani Santos[a,b], Luk Rombauts[e,g], Alberto Rosello-Diez[h,i,j], and Evdokia Dimitriadis[a,b,c,2]

Affiliations are included on p. 11.

Edited by Janet Rossant, Gairdner Foundation, Toronto, ON, Canada; received January 24, 2024; accepted September 5, 2024

The endometrium undergoes substantial remodeling in each menstrual cycle to become receptive to an implanting embryo. Abnormal endometrial receptivity is one of the major causes of embryo implantation failure and infertility. MicroRNA-124-3p is elevated in both the serum and endometrial tissue of women with chronic endometritis, a condition associated with infertility. MicroRNA-124-3p also has a role in cell adhesion, a key function during receptivity to allow blastocysts to adhere and implant. In this study, we aimed to determine the function of microRNA-124-3p on endometrial epithelial adhesive capacity during receptivity and effect on embryo implantation. Using a unique inducible, uterine epithelial-specific microRNA overexpression mouse model, we demonstrated that elevated uterine epithelial microRNA-124-3p impaired endometrial receptivity by altering genes associated with cell adhesion and polarity. This resulted in embryo implantation failure. Similarly in a second mouse model, increasing microRNA-124-3p expression only in mouse uterine surface (luminal) epithelium impaired receptivity and led to implantation failure. In humans, we demonstrated that microRNA-124-3p was abnormally increased in the endometrial epithelium of women with unexplained infertility during the receptive window. MicroRNA-124-3p overexpression in primary human endometrial epithelial cells (HEECs) impaired primary human embryo trophectoderm attachment in a 3-dimensional culture model of endometrium. Reduction of microRNA-124-3p in HEECs from infertile women normalized HEEC adhesive capacity. Overexpression of microRNA-124-3p or knockdown of its direct target *IQGAP1* reduced fertile HEEC adhesion and its ability to lose polarity. Collectively, our data highlight that microRNA-124-3p and its protein targets contribute to endometrial receptivity by altering cell polarity and adhesion.

endometrial receptivity | endometrial epithelium | microRNA | miR-124-3p | embryo implantation

Significance

Uterine receptivity is essential for embryo implantation and successful pregnancy. Failed implantation due to impaired uterine receptivity significantly contributes to infertility, yet no tests currently identify endometrial-driven infertility. In this study, we demonstrated that microRNA-124-3p is abnormally elevated in the uterine epithelium of women with infertility during the receptive phase. We developed two models: a genetically inducible, uterine epithelium-specific microRNA-124-3p overexpression mouse model and a 3-dimensional human embryo trophectoderm-endometrial cell coculture model. Using these models, we showed that elevated microRNA-124-3p in both mice and humans disrupted endometrial epithelial cell adhesion and polarity, preventing the uterine epithelium from transitioning to a receptive state. This research identifies microRNA-124-3p as a diagnostic and therapeutic target for endometrial-driven infertility.

The human endometrium undergoes substantial remodeling during each menstrual cycle to become receptive to an implanting embryo only within a narrow window of 2 to 4 d in the mid-secretory phase (1, 2). Inadequate remodeling of endometrium during receptivity is a major cause of embryo implantation failure and female infertility (3). The importance of a receptive uterus for embryo implantation in vivo has been proven by animal models (4). Using reciprocal embryo transfer in rats and mice, it has been shown that blastocysts cannot implant and will degenerate outside the receptive window (5, 6). To attain receptivity the endometrial luminal epithelium must lose its polarity and an apical surface that is repulsive toward the polarized blastocyst trophectoderm (7–9). This allows firm attachment and adhesion between the trophectoderm and luminal epithelium, initiating implantation (3). Inadequate remodeling of the endometrial luminal epithelium results maintenance of polarity, preventing embryo attachment and implantation (9–11). Remodeling of the luminal epithelium involves changes in the expression of adhesive molecules on the apical surface and alterations in cell polarity. However, the mechanisms enabling these changes remain elusive.

MicroRNAs (miRs) are dysregulated in the receptive endometrium of women with infertility (12–14). The regulation of protein translation by miRs is an efficient mechanism to control multiple protein-coding genes that may be necessary for specific cell functions. miRs disrupt gene/protein expression by destabilizing the transcript or repressing translation initiation (15, 16). Consequently, dysregulation of a single miR can disrupt the expression of multiple genes/proteins and significantly impact endometrial epithelial function within a short time window (17). However, there is limited evidence on how individual miRs that are dysregulated in endometrial epithelium of women with primary infertility during receptivity contribute to endometrial receptivity.

The authors declare no competing interest.

This article is a PNAS Direct Submission.

[1]W.Z. and M.V.S. contributed equally to this work.

[2]To whom correspondence may be addressed. Email: evdokia.dimitriadis@unimelb.edu.au.

This article contains supporting information online at https://www.pnas.org/lookup/suppl/doi:10.1073/pnas.2401071121/-/DCSupplemental.

Published October 4, 2024.

miR-124-3p has been reported to be elevated in both endometrial tissue and serum of women with chronic endometritis during receptivity (18), a condition associated with infertility and chronic inflammation. miR-124-3p is predicted to regulate genes in the endometrial luminal epithelium vital for endometrial receptivity including leukemia inhibitory factor (*LIF*) and signal transducer and activator of transcription 3 (*STAT3*) (19–21). In cancer cells, miR-124-3p can suppress cell adhesive capacity and invasiveness (22, 23), processes known to dysregulate endometrial receptivity. Therefore, in this study, we aimed to investigate the role of miR-124-3p in endometrial receptivity and embryo implantation by focusing on epithelial cell remodeling, as the initiation of implantation depends on the firm adhesion of the blastocyst trophectoderm to the endometrial luminal epithelium.

In this study, we developed and used an inducible, uterine epithelial-specific miR-124-3p overexpression mouse model (transgenic miR-124-3p mice). We determined that uterine epithelial-specific overexpression of miR-124-3p compromised epithelial cell remodeling and receptivity, resulting in implantation failure without affecting blastocysts. In humans, we demonstrated that miR-124-3p was abnormally elevated in the endometrial luminal epithelium of patients with primary unexplained infertility, many of whom exhibit dysregulated receptivity (24). Using four independent in vitro human models, we demonstrated that miR-124-3p negatively affected the adhesive capacity of endometrial epithelial cells. We found that miR-124-3p overexpression in endometrial epithelial cells impaired human embryo trophectoderm adhesion to a 3-D primary human endometrial epithelial-stromal cell bilayer. Mechanistically, overexpression of miR-124-3p disrupted the endometrial epithelial cell changes necessary for adhesion and polarity required for receptivity in both mice and humans. Overall, our findings provide strong evidence that dysregulation of miR-124-3p can block endometrial epithelial cell function during receptivity, leading to implantation failure.

Results

Inducing Overexpression of miR-124-3p in the Uterine Epithelium During the Receptive Window Blocks Receptivity and Leads to Implantation Failure. To determine whether luminal epithelial expression of miR-124-3p was associated with receptivity we examined its expression in mice just before and during the receptive period. Luminal epithelial miR-124-3p production was significantly down-regulated in the receptive phase (day of implantation, embryonic day [E]4) (day of plug designated E0) compared to the previous day (E3) (Fig. 1*A*). This suggested that miR-124-3p needs to be reduced in the luminal epithelium during receptivity to enable blastocyst attachment and initiate implantation. To test this, we generated an inducible, uterine epithelium-specific miR-124-3p overexpression mouse model. We used the doxycycline-controlled and cre recombinase activated gene overexpression (Dragon) system (*Materials and Methods*) (25). Briefly, three transgenic mice were crossed to create transgenic miR-124-3p mice [*Ltf-Cre*+ (26), *CAG-rtTA3*+ (27), *Dragon-miR-124-3p*+]. Activation of the Dragon-miR-124-3p allele and therefore miR-124-3p overexpression depends on both iCre and rtTA3 drivers, such that overexpression only occurs in tissues/cells where both drivers overlap and doxycycline is present (*SI Appendix*, Fig. S1).

To overexpress miR-124-3p during receptivity, doxycycline was given by intraperitoneal injection every 12 h between E2 9 pm and E4 9 am (Fig. 1*B*). qPCR analysis identified that mature miR-124-3p was overexpressed in the uterus of transgenic miR-124-3p mice (Fig. 1*C*). We found that miR-124-3p overexpression significantly reduced the number of implantation sites in the transgenic miR-124-3p mice compared to control (Fig. 1*D*, $P < 0.0001$). The levels of miR-124-3p overexpression were positively correlated with the severity of implantation outcomes, as implantation was completely blocked in the two mice with over 10-fold increase of miR-124-3p (Fig. 1*C*, arrows). In situ hybridization confirmed that miR-124-3p overexpression was localized specifically to the uterine luminal and glandular epithelium in the transgenic miR-124-3p mice (n = 3, Fig. 1*E*). For the few embryos that implanted in the transgenic mouse uterus [total of four implantation sites in five mice (Fig. 1*D*)], their viability was confirmed by the absence of cleaved Caspase-3 staining (Fig. 1*F*).

miR-124-3p Targets a Wide Range of Receptivity-Related Genes in Transgenic miR-124-3p Mouse Uteri. To determine the gene targets affected by miR-124-3p overexpression during endometrial receptivity, we analyzed E4.5 uteri (just postembryo attachment) from both transgenic control and miR-124-3p mice. qPCR analysis of selected epithelial receptivity markers (*Areg*, *Muc1*, and *E-cadherin*) and stromal decidualization markers (*Bmp2*, *Hand2*, and *Cox2*) revealed significant differences between transgenic control and miR-124-3p mice (Fig. 2*A*). We therefore expanded the investigation of genes altered in the transgenic miR-124-3p mice using a customized PCR array containing 83 receptivity-associated genes in mice (Dataset S1) (28). Among them, 38 genes showed significant differences in expression in the miR-124-3p overexpression uterus compared to control (Fig. 2*B*). Furthermore, 29 genes were significantly reduced by miR-124-3p overexpression in the uterus at E4.5 compared to transgenic control mice (Fig. 2*B*). This included genes known to regulate endometrial receptivity (*Hoxa11*, *Egf*, *Areg*, *Ptgs2*), extracellular matrix/cell adhesion molecules (*Sparc*, *Gpx3*, *Col5a2*, *Vcan*, *Itga5*, *Snai2*), postimplantation genes (*Vegfa*, *Mid1*, *Timp1*), cytokines (*Il15*, *Il11*), leukocyte migration (*Mmp2*, *Fbn1*, *Icam1*, *Lama1*), cell cycle (*Pcna*, *Stmn1*, *Mki67*, *Ccnb1*), and signal transduction (*Ctnnb1*, *Il1r1*, *Sfrp4*, *Trp53*, *Il1a*). These data suggest that embryos did not firmly adhere to the endometrial luminal epithelium to initiate implantation and the decidual response. miRs act by destabilizing mRNA or repressing mRNA translation, leading to downregulation of target proteins. Here, we confirmed bioinformatically that 21 of the 29 genes reduced have miR-124-3p binding sites (bolded in Fig. 2*B*) suggesting that they may be direct targets. Conversely the expression of nine genes was significantly increased after miR-124-3p overexpression (*Esr1* to *Gdf15* in Fig. 2*B*) suggesting that they may be indirect targets.

miR-124-3p Overexpression in the Endometrial Epithelium Compromises Implantation Chamber Formation and the Loss of Luminal Epithelial Cell Polarity. Since implantation occurred in some transgenic miR-124-3p mice [a total of four implantation sites in five mice (Fig. 1*D*)], when examining mouse uteri by immunohistochemistry, we divided transgenic miR-124-3p mouse uteri into two subgroups: areas with and without implantation sites. Morphologically, the uterine lumen failed to close properly in the implantation sites from transgenic miR-124-3p mice (Fig. 2 *C*, *Middle* panel). Staining of SCRIBBLE and E-cadherin identified retention of cell polarity in the luminal epithelium in both areas with implantation sites and without implantation site groups in transgenic miR-124-3p mice. This is in contrast to normal pregnancy where uterine luminal epithelial cell polarity should be minimized to allow close contact to the polarized embryo surface (9, 29) (Fig. 2 *C*, *Top* panel). While there was no difference in localization and staining intensity in areas with implantation sites

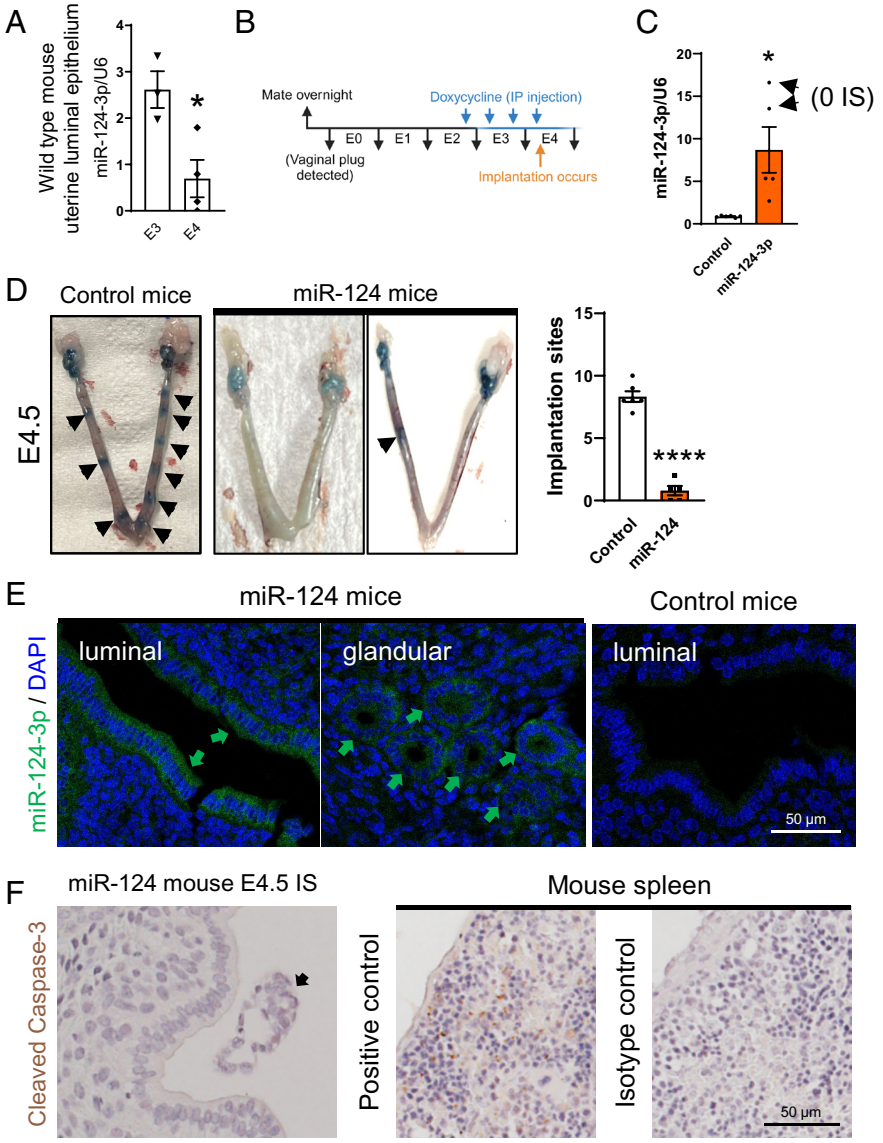

Fig. 1. Overexpression of miR-124-3p in the murine uterine epithelium during endometrial receptivity impaired implantation. (*A*) Endogenous miR-124-3p levels in uterine luminal epithelium from pregnant wildtype mouse uterine luminal epithelium at E3 and E4 (qPCR; N = 3 to 4). (*B–F*) Uterine epithelium specific miR-124-3p overexpression significantly reduced implantation success in mice. (*B*) Timeline of doxycycline treatment to induce miR-124-3p overexpression during endometrial receptivity. (*C*) miR-124-3p overexpression in the uterus was verified at E4.5 by qPCR (N = 5 to 6). *(D)* miR-124-3p overexpression significantly reduced implantation site number (IS, arrowhead) at E4.5 (N = 5 to 6). (*E*) miR-124-3p overexpression was localized to the luminal and glandular epithelium by in situ hybridization. (*F*) miR-124-3p did not affect embryo viability, IS found in transgenic miR-124-3p mice stained with the cell apoptosis marker Cleaved Caspase-3. Wildtype mouse spleen was used as a positive control for staining. All data are presented as mean ± SEM. *$P < 0.05$, ****$P < 0.0001$.

between transgenic control and miR-124-3p mice, in miR-124-3p mouse uteri without implantation sites, there was no detectable staining for P-STAT3, DESMIN, and KI-67 staining (Fig. 2*C*), suggesting that where the embryo was present, decidual changes associated with implantation were capable of being initiated.

Overexpression of miR-124-3p Specifically in the Mouse Uterine Luminal Epithelium Impairs Receptivity. Our overall aim was to investigate how changes in the uterine luminal epithelium during receptivity impacted embryo attachment and implantation. Since our transgenic mouse model overexpressed miR-124-3p in both luminal and glandular epithelium, we used intrauterine injection to selectively deliver and overexpress AgomiR-124-3p specifically to the luminal epithelium. Briefly each mouse received intrauterine injections to one horn of either AgomiR-124-3p or a control AgomiR mimic at E3, with each mouse therefore serving as both a treatment and control (Fig. 3*A*). qPCR analysis confirmed a significant fourfold increase in miR-124-3p expression levels in the luminal epithelium at E4 following intrauterine injection compared to AgomiR-control ($P < 0.05$, Fig. 3*B*). No significant change in miR-124-3p levels was observed in the remaining uterus (Fig. 3*B*). In situ hybridization also confirmed that miR-124-3p overexpression was confined to the uterine luminal epithelium (Fig. 3*C*). Treatment with AgomiR-124-3p significantly reduced ($P < 0.01$) implantation site number compared to AgomiR-control treatment (Fig. 3*D*), with five of eight treated mice having no implantation sites in the AgomiR-124-3p treated horn. To confirm that miR-124-3p did not affect embryo viability we transfected wildtype mouse embryos in vitro with miR-124-3p mimic. There was no effect on embryo zona pellucida breaking/demise, hatching, and outgrowth, compared to control (Fig. 3*E* and *SI Appendix*, Fig. S2). Therefore, the compromised implantation was likely caused by altered miR-124-3p effects on uterine epithelium during receptivity.

In uterine horns treated with AgomiR-124-3p where implantation sites were absent, we observed that the luminal epithelium maintained

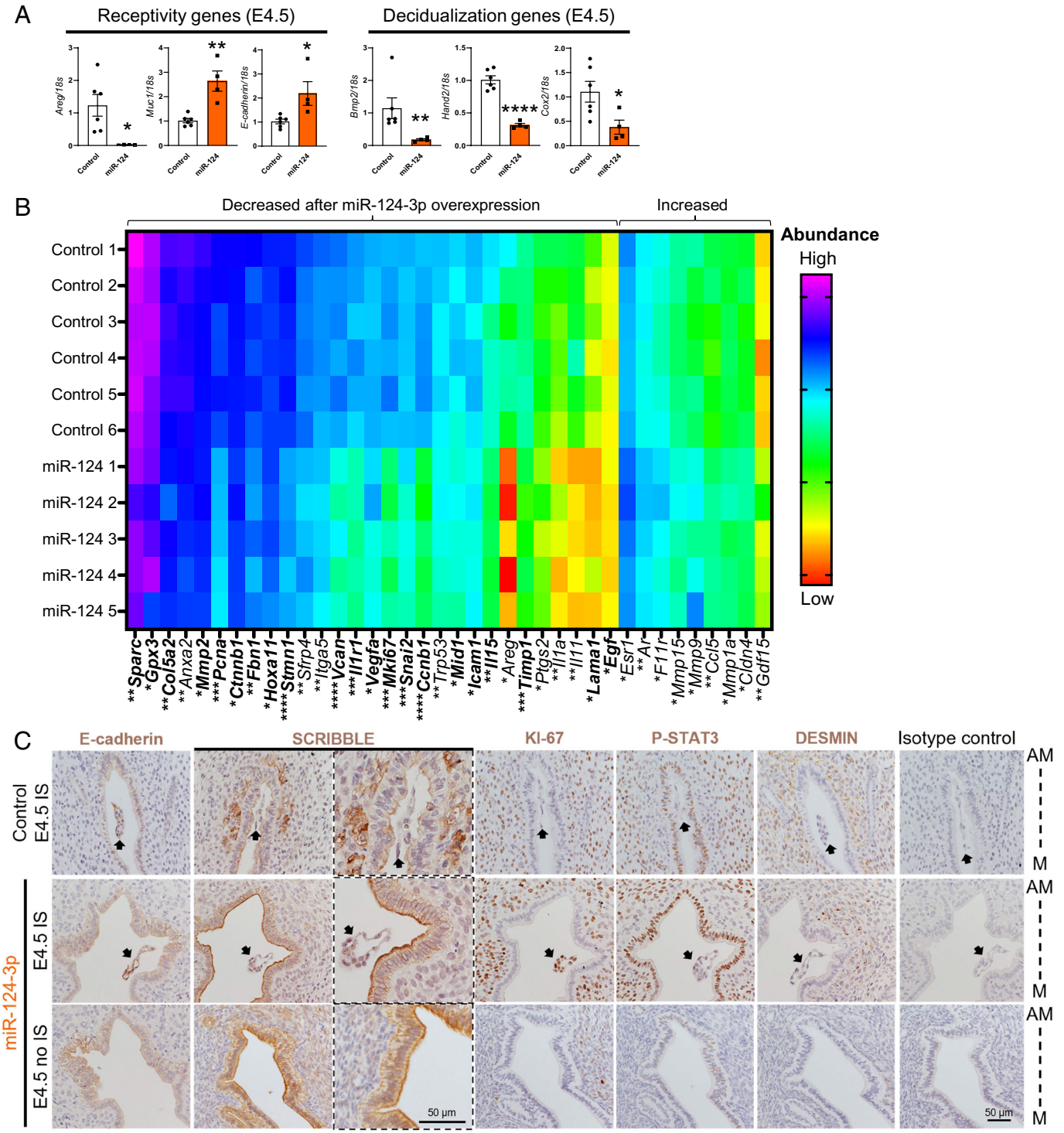

Fig. 2. miR-124-3p overexpression in mouse uterine epithelium impairs receptivity. (*A*) Representative receptivity and decidualization genes in E4.5 transgenic control and miR-124-3p uteri (qPCR; N = 4 to 6). All data are presented as mean ± SEM. (*B*) Heatmap of results from customized PCR gene array on E4.5 uteri from transgenic miR-124-3p and control mice. Data presented as dCt value in heat map and ranked by expression level (high to low) (N = 5 to 6). Genes having miR-124-3p binding site(s) highlighted in bold. Original data provided in Dataset S1. *$P < 0.05$, **$P < 0.01$, ***$P < 0.001$, ****$P < 0.0001$. (*C*) Immunohistochemistry staining at E4.5 of cell polarity markers (E-cadherin, SCRIBBLE), proliferation marker (KI-67), receptivity marker (P-STAT3), and decidualization marker (DESMIN). As no implantation sites were recorded in some miR-124-3p transgenic mice, uteri at E4.5 were also stained. Arrow: implanting blastocyst. The tissue sections are oriented so that the antimesometrial (AM) sides of the uterus is at the top and the mesometrial (M) is at the bottom.

its cell polarity, as revealed by SCRIBBLE staining (Fig. 3 *F*, *Top* panel), and no decidualization response occurred, as indicated by SCRIBBLE and DESMIN staining (Fig. 3*F*). Overexpression of miR-124-3p specifically in the uterine luminal epithelium resulted in a significant reduction in the expression of implantation-related genes *Bmp2*, *Wnt4*, *Hand2*, and *Cox2* (30–33) compared to AgomiR-control (Fig. 3*G*), confirming that the embryo failed to firmly attach and initiate implantation, and that the decidualization response was impaired. By contrast, in uterine horns treated with AgomiR-124-3p where implantation sites were present, we saw no differences in the localization and intensity of SCRIBBLE and DESMIN staining compared to AgomiR-control (Fig. 3*F*). The uterine lumen remained closed in the AgomiR-124-3p treated group with implantation sites, similar to AgomiR-control (Fig. 3*F*).

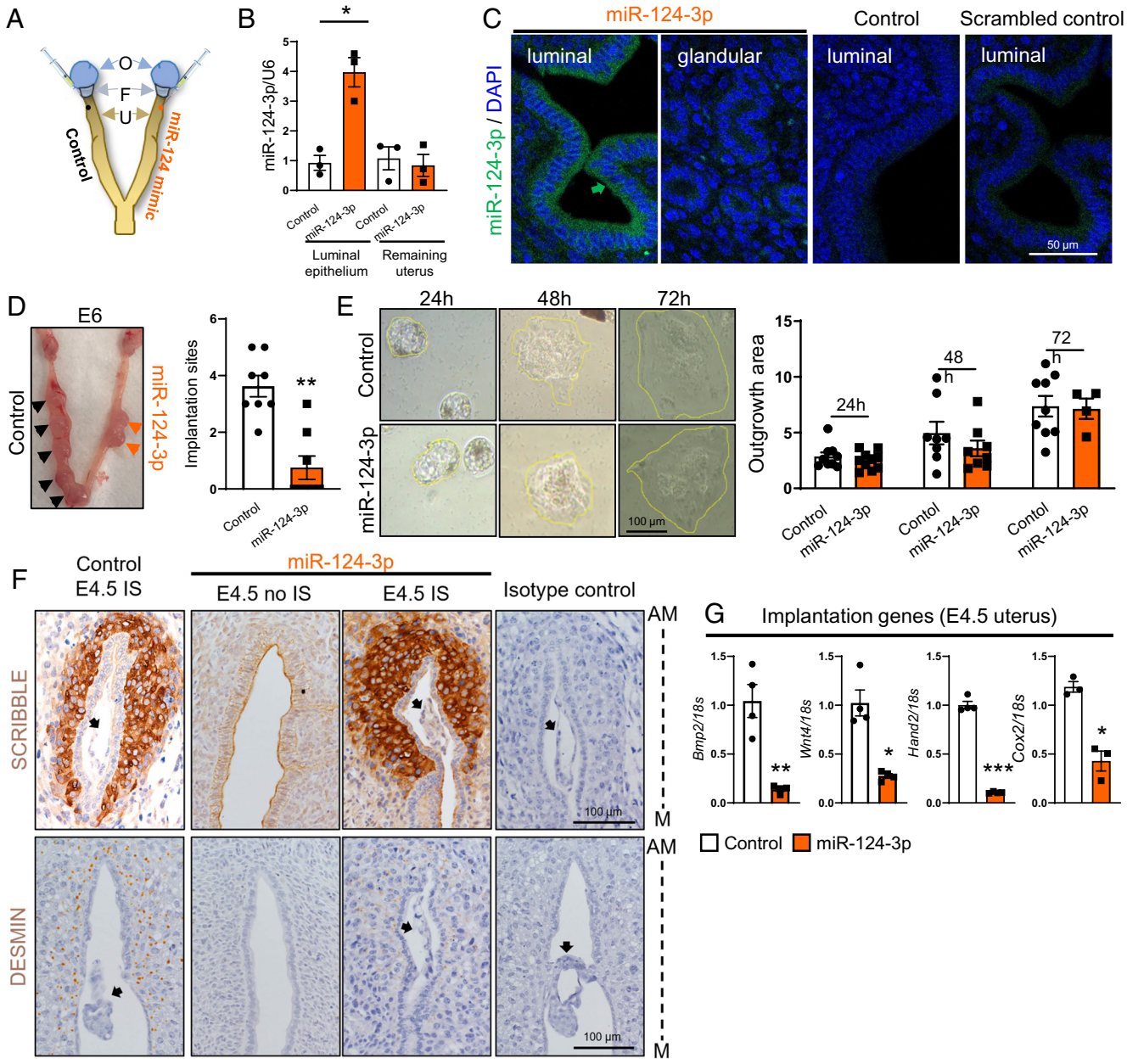

Fig. 3. Luminal epithelium only miR-124-3p overexpression impaired implantation. (*A*) Schematic diagram of the intrauterine injection to overexpress miR-124-3p in the mouse luminal epithelium. For each individual mouse, AgomiR-124-3p or scrambled mimic was injected into one side of the uterine horn at E3. O: Ovary, F: Fallopian tube, U: Uterus. (*B*) miR-124-3p was significantly elevated in the luminal epithelium after intrauterine injection compared to the remaining uterus and control uterine horn (qPCR; N = 3). (*C*) miR-124-3p overexpression localized to the luminal epithelium as determined by in situ hybridization. (*D*) Intrauterine injection of miR124-3p significantly reduced implantation site number in the treated horn compared to untreated control at E6 (N = 8). (*E*) Exposure of unhatched wildtype mouse embryos at E4 to miR-124-3p showed no effect on outgrowth compared to control. (*F* and *G*) The effect of miR-124-3p overexpression on receptivity and decidualization markers was determined by immunohistochemistry (*F*) and qPCR (*G*). Arrow: implanting blastocyst (N = 3 to 4). The tissue sections are oriented so that the AM sides of the uterus is at the top and the M is at the bottom. All data are presented as mean ± SEM. **P* < 0.05, ***P* < 0.01, ****P* < 0.001, IS: implantation site.

miR-124-3p Expression Is Elevated in the Endometrium of Women with Primary Infertility. To investigate the clinical relevance of miR-124-3p on endometrial function, its expression was assessed in endometrial tissues across the menstrual cycle from women with normal fertility (fertile) and women with primary unexplained infertility (infertile). miR-124-3p was expressed in all phases of the menstrual cycle in both fertile and infertile groups (Fig. 4*A*). qPCR analysis identified that in fertile women, miR-124-3p expression decreased during the secretory phase compared to the proliferative phase, particularly during the mid-secretory phase (Fig. 4*A*). This decrease was not observed in infertile women and miR-124-3p expression was significantly increased in infertile endometrium compared to fertile endometrium during the early and mid-secretory phases (Fig. 4*A*). In situ hybridization of mid-secretory phase endometrium illustrated miR-124-3p localization in the luminal and glandular epithelium of infertile endometrium, whereas minimal fluorescence was observed in the fertile endometrium (Fig. 4*B*). Overall, these findings suggest that miR-124-3p expression is dysregulated in infertile endometrium.

Overexpression of miR-124-3p in Human Endometrial Epithelial Cells Impairs Their Adhesive Capacity and Receptivity. To explore how miR-124-3p overexpression affects endometrial epithelial cell adhesive capacity and receptivity, we employed a

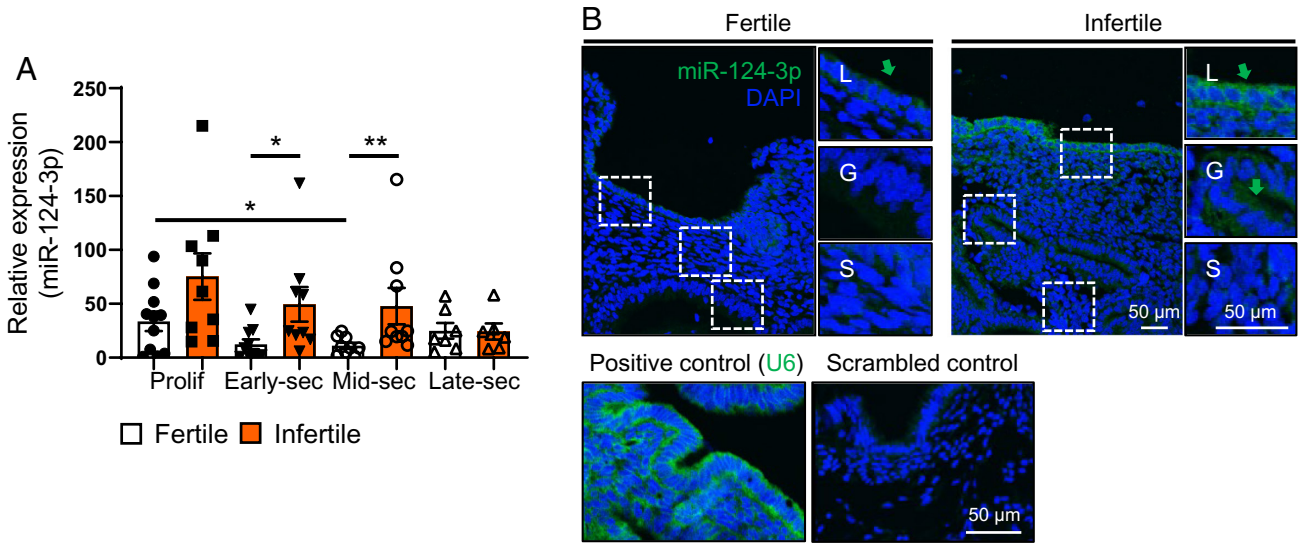

Fig. 4. miR-124-3p was overexpressed in infertile human endometrial luminal epithelium during receptive phase. (*A*) miR-124-3p expression in endometrial tissue (qPCR; N = 6 to 11) from fertile and infertile endometrium. Expression levels were normalized to U44. The unpaired *t* test was used to compare miR-124-3p levels between each phase and between fertile and infertile groups. Data are presented as mean ± SEM. *$P < 0.05$, **$P < 0.01$. (*B*) In situ hybridization of miR-124-3p on mid-secretory phase endometrial sections revealed strong fluorescence in the luminal epithelial cells of the infertile endometrium, compared to fertile endometrium (green arrows, N = 3). Sections were counterstained with DAPI to reveal the cell nuclei (blue). As controls, endometrial sections were either incubated with U6 probe (positive control) or scrambled sequence probe (scrambled control). L: Luminal epithelium; G: Glandular epithelium; S: Stroma.

3D model mimicking implantation. This model consisted of a layer of primary human endometrial epithelial cells (HEECs) placed on top of a layer of primary human endometrial stromal cells, isolated from women with normal fertility, as previously described with some modifications (34). Initially miR-124-3p was overexpressed in HEECs before they were overlaid on the primary human endometrial stromal cell layer to form a bilayer construct. Primary human embryo trophectoderm spheroids were prepared from Day 6 embryos by removing the inner cell mass (Fig. 5*A*). The trophectoderm were allowed to reform spheroids for up to 2 h (Fig. 5*B*). The re-expanded trophectoderm spheroids were added to endometrial constructs and monitored for their ability to firmly adhere to the endometrial epithelium and to outgrow for up to 120 h (equivalent to Day 11 postfertilization embryo).

Control group trophectoderm spheroids firmly attached within 48 h and continued to grow until 120 h (Fig. 5*C*). Human chorionic gonadotropin (hCG) was detected in the coculture media by ELISA, with an average concentration of 7,040 ± 569 pg/mL at 120 h (N = 3). However, in the miR-124-3p group, all three trophectoderm spheroids failed to firmly attach to the endometrial constructs within 48 h, and two of them showed reduced trophectoderm area and signs of degeneration before 72 h of culture. Only one trophectoderm spheroid could be traced until 120 h, but it appeared to degenerate by 72 h, with very few trophectoderm cells remaining visible by 120 h (Fig. 5*C*). hCG was undetectable in the coculture media from the miR-124-3p group at 72 and 120 h. Overall, our data indicate that miR-124-3p overexpression in HEECs impaired trophectoderm spheroid attachment, likely leading to cell death or apoptosis.

To further understand the impact of miR-124-3p overexpression on embryo adhesion we used two additional in vitro human models. Primary trophectoderm was replaced with HTR8/SVneo (trophoblast cell line) spheroids and their adhesion on either the 3D endometrial construct or a HEEC monolayer was determined. Both models confirmed that miR-124-3p overexpression in fertile HEECs significantly impaired ($P < 0.05$) their adhesiveness to HTR8/SVneo spheroids (Fig. 5 *D* and *E*).

By comparison to fertile HEECs, the levels of miR-124-3p were significantly elevated in infertile HEECs ($P < 0.05$, Fig. 5*F*). To investigate whether miR-124-3p inhibition can improve cell adhesive capacity of infertile HEECs, HEECs from infertile women were transfected with a miR-124-3p inhibitor. Following miR-124-3p inhibitor treatment, the adhesive capacity of infertile HEECs to HTR8/SVneo spheroids significantly increased ($P < 0.01$, Fig. 5*G*) compared to the control. As the fourth model to assess the adhesive ability of endometrial epithelial cells without using spheroids, Ishikawa cells [a receptive endometrial epithelial cell line (35)] were investigated by xCELLigence to monitor the effects of elevated miR-124-3p on their adhesive capacity in real-time. miR-124-3p mimic treatment of Ishikawa cells significantly reduced their adhesion at 2 h ($P < 0.0001$) and was reversed after cotreatment with the miR-124-3p inhibitor (*SI Appendix*, Fig. S3).

miR-124-3p Targets Adhesion Related Molecules in HEECs. As endometrial epithelial cells must remodel in the receptive phase to facilitate embryo adhesion and initiate implantation, we investigated putative miR-124-3p targets with known functions on cell adhesion. 88 genes (Dataset S2) were identified and screened in HEECs via the Fluidigm BioMark HD System. The list included genes with confirmed functions in regulating embryo implantation in mice (e.g., *STAT3* and *JAG*) (28, 36) and target genes that have not been investigated in endometrial receptivity (e.g., *IQGAP1*). Of the 88 genes, 20 were significantly downregulated following miR-124-3p overexpression in HEECs compared to control (Fig. 6*A*). Nine of the 20 miR-124-3p targets identified in HEECs were similarly downregulated in E4.5 transgenic miR-124-3p mouse uterus, suggesting similar mechanisms of action in the epithelium between the two species (Fig. 6*B*).

IQGAP1 was selected for further investigation due to its unknown function in endometrial epithelial cell adhesion. To determine the clinical relevance of IQGAP1 in endometrial receptivity, the localization and production levels of IQGAP1 in the receptive phase endometrium were compared between fertile and infertile women. IQGAP1 localized to the luminal epithelium, glandular epithelium, and stromal cells (Fig. 7*A*). The staining

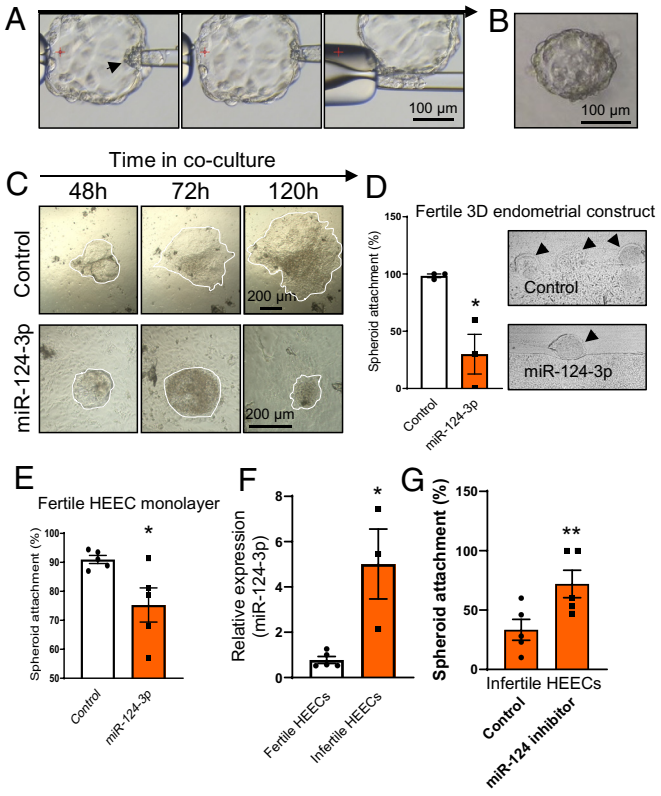

Fig. 5. miR-124-3p impaired HEEC receptivity. (*A–C*) Outgrowth of primary human trophectoderm spheroids on a 3D primary human endometrial cell construct. Primary HEECs in the construct were transfected with miR-124-3p mimic or scrambled control (N = 3). (*A*) Before culture, inner cell mass (arrow) was removed from day 6 human blastocysts. (*B*) The remaining blastocyst readily re-formed into a spheroid. (*C*) Human trophectoderm attachment and outgrowth on the 3D endometrial construct (outlined, cultured up to 120 h) (N = 3). (*D* and *E*) Adhesion of HTR8/SVneo spheroid to (*D*) 3D endometrial construct (N = 3) or (*E*) HEEC monolayer (N = 3 to 5). (*F*) miR-124-3p levels in fertile and infertile HEECs (N = 3 to 5). (*G*) HTR8/SVneo spheroid adhesion to infertile HEECs transfected with miR-124-3p inhibitor or control (N = 5). Data are presented as mean ± SEM. **P* < 0.05, ***P* < 0.01.

intensity of IQGAP1 was significantly higher in all cellular compartments in the fertile endometrium compared to the infertile group (Fig. 7 *A* and *B*).

In HEECs, our results confirmed that miR-124-3p overexpression significantly downregulated IQGAP1 protein levels compared to control ($P < 0.01$, Fig. 7*C*). Knockdown of *IQGAP1* in HEECs significantly compromised their adhesiveness to HTR8/SVneo spheroids compared to control (Fig. 7 *D* and *E*). To explore the direct interaction between miR-124-3p and *IQGAP1* in HEECs, we applied a "TSB" designed to bind specifically to the miR-124-3p target site of the *IQGAP1* mRNA (Fig. 7*F*), thereby blocking miR-124-3p accessing that site. As expected, cotransfection of HEECs with miR-124-3p and the *IQGAP1* TSB significantly increased production of IQGAP1 compared to HEECs transfected with miR-124-3p alone (Fig. 7*G*, $P < 0.01$). Similarly, treatment with the TSB restored HEEC adhesive capacity to HTR8/SVneo spheroids (Fig. 7*H*, $P < 0.05$). MiR-124-3p overexpression in both human and mouse models significantly reduced *Iqgap1* expression (Figs. 6*B* and 7*I*), suggesting *IQGAP1* is a common miR-124-3p target between humans and mice.

miR-124-3p and IQGAP1 Regulate the Polarity of HEECs. IQGAP1 engages with cytoskeleton proteins to internalize cadherin junction protein E-cadherin in human mammary glandular epithelial cells (37). Here, we sought to test whether IQGAP1 reduces endometrial epithelial cell polarity by internalizing E-cadherin. We first confirmed the reduction of IQGAP1 protein in Ishikawa cells after transfection with either *IQGAP1* siRNA or miR-124-3p mimic (Fig. 8*A*, $P < 0.05$). Using a transepithelial electrical resistance assay, we demonstrated that loss of IQGAP1 in Ishikawa cell monolayers (either by *IQGAP1* siRNA or miR-124-3p mimic treatment, Fig. 8*B*) increased transepithelial electrical resistance, therefore increasing cell polarity (38) at 72 h posttransfection ($P < 0.05$) compared to control. In agreement, confocal scanning of the entire lateral layer of the Ishikawa monolayers revealed loss of IQGAP1 resulted in the retention of E-cadherin on the cell lateral surface and the cell polarity marker SCRIBBLE compared to controls (Fig. 8*C*).

Discussion

Endometrial receptivity involves the dramatic remodeling of all cellular compartments in the endometrium and is widely recognized to be critical for embryo implantation and the establishment of pregnancy (3, 4). However, how endometrial epithelial cell adhesive capacity during receptivity is regulated in humans remains largely elusive. In this study, we identified elevated levels of miR-124-3p in the endometrial epithelium of women with unexplained infertility. We aimed to investigate the role of miR-124-3p in regulating endometrial epithelial cell adhesive capacity and its subsequent effect on embryo implantation in a unique way. This was achieved by developing a genetically inducible mouse model to overexpress miR-124-3p specifically within the uterine epithelium during the receptive window. This approach allowed us to explore the impact of miR-124-3p on endometrial adhesive capacity and receptivity in a controlled manner. This finding represents a significant advancement in our understanding of how dysregulation of miRs can affect endometrial receptivity and lead to implantation failure.

Using genetic mouse models, studies have provided fundamental information on key uterine genes regulating embryo implantation. Among pioneering examples (39), maternal deletion of *Cox2* leads to implantation failure by blocking blastocyst attachment and decidualization (30) while uterine knockout of *Bmp2* only affects decidualization (31). Using genetic mouse models to determine miR functions on embryo implantation is rare, previous studies have relied on intrauterine injection of miR mimics (40) which may not accurately represent miR dysregulation in vivo because it bypasses endogenous transcriptional modification and may have unintended off target effects on the uterus. To complement intrauterine injection, here we used a combination of Cre-Loxp and Tet-on systems to genetically overexpress miR-124-3p specifically in the uterine epithelium during the receptive window. This study achieves miR overexpression in a cell-type-specific and time-dependent manner in the uterus. Our findings suggest that there is a critical time window during which miR-124-3p levels in the uterine epithelium need to be downregulated to facilitate implantation. Despite our genetic approach we still found variability in the levels of overexpression achieved, suggesting heterogeneity in the activation and/or turnover of miRs between animals and within the uterus. In addition, we recorded inconsistent results regarding implantation chamber formation in the intrauterine injection model. A potential reason for this is the inherent limitation of intrauterine injection which could fail to uniformly distribute miR-124-3p mimic across the entire uterine luminal surface. Overall, by using these two models, we were able to overexpress miR-124-3p in the luminal and glandular epithelium or in the luminal epithelium only. Increasing miR-124-3p only in the luminal epithelium was sufficient to block almost all

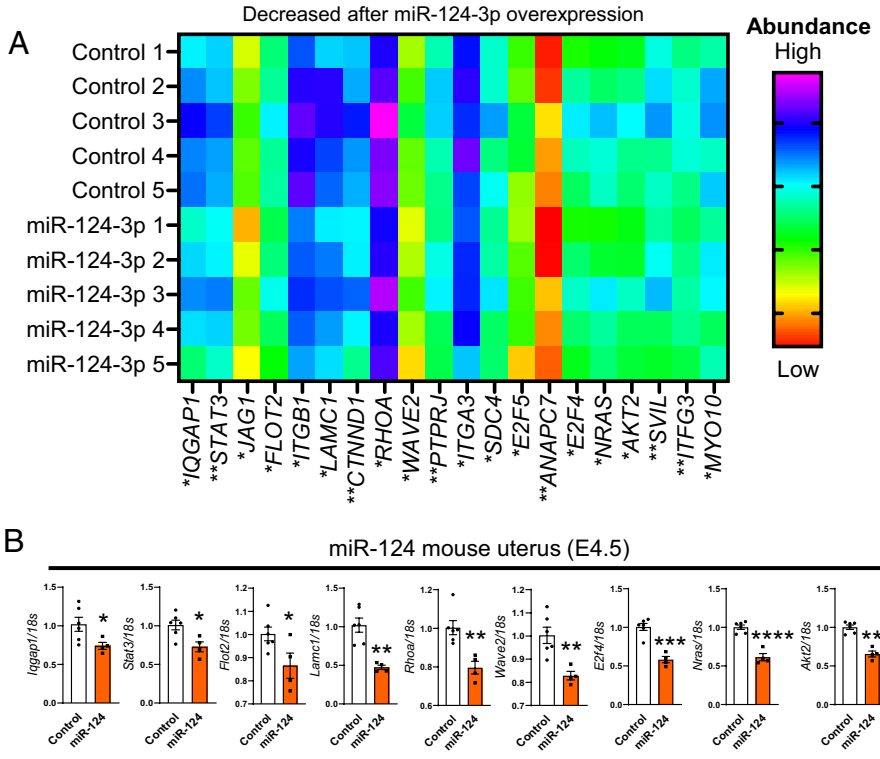

Fig. 6. miR-124-3p targets adhesion genes in human and mouse uterus. (*A*) Fluidigm BioMark HD System was applied to quantify the expression of 88 genes in HEECs transfected with scrambled control or miR-124-3p mimic. These genes are predicted miR-124-3p targets and fall into broad categories of cell adhesion and attachment. Data were presented as dCt value in heat map (N = 5). Original data provided in Dataset S2. (*B*) Expression of miR-124-3p gene targets identified in *A* in E4.5 uterus from transgenic miR-124-3p or control mice (N = 4 to 6). Data are presented as mean ± SEM. **P* < 0.05, ***P* < 0.01, ****P* < 0.001, **** *P* < 0.0001.

embryo implantation. In both models however, where implantation occurred the decidual response was initiated as expected.

In mice, blastocysts enter the uterus from the oviduct on the morning of E3 (E0 designated as morning of plug detection) and rapidly distribute themselves evenly along the uterine horn within a few hours (41). During this period, the uterus must be refractory to prevent early attachment which would result in all blastocysts being clustered together near the oviduct (42). We recorded a

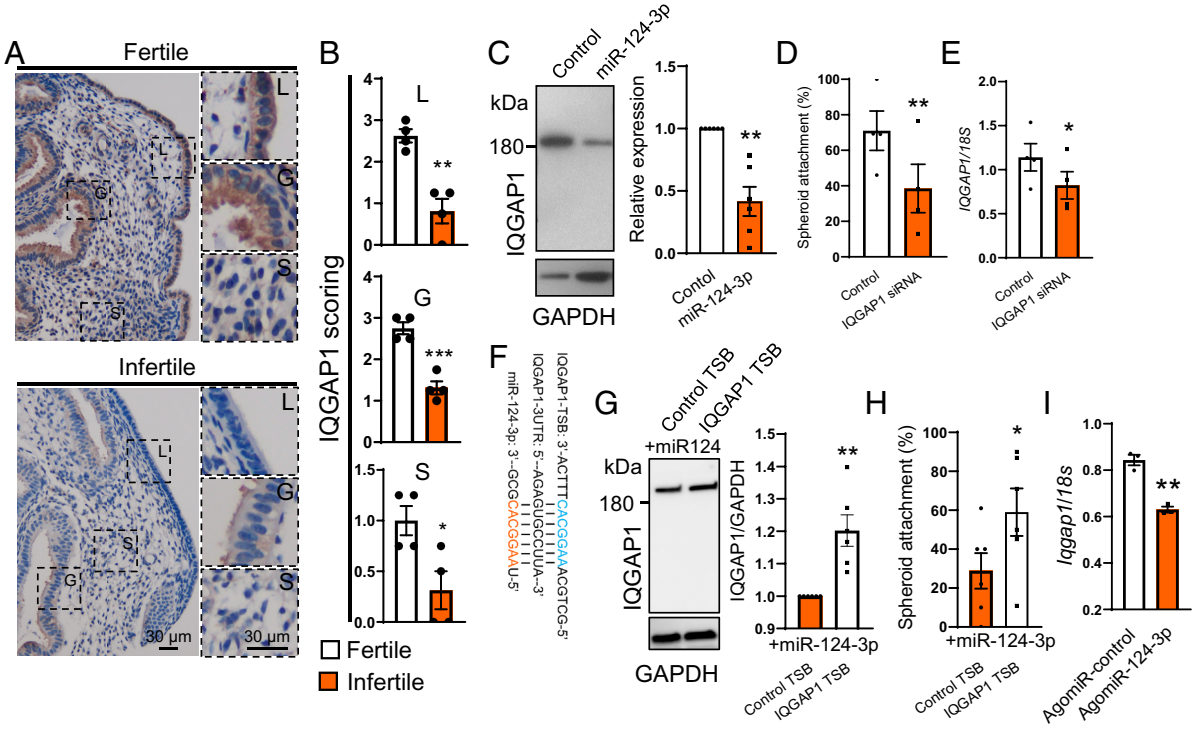

Fig. 7. miR-124-3p target *IQGAP1* alters HEEC adhesion. (*A* and *B*) IQGAP1 immunolocalization in fertile and infertile secretory phase human endometrium. Higher magnification images of the luminal epithelium (L), glandular epithelium (G), and stromal cells (S) are depicted on the right of panels with their original locations indicated by outlines on the left. Sections were counterstained with hematoxylin to indicate cell nuclei (blue). IQGAP1 staining intensity (N = 4) was semiquantitated by scoring. Endometrial tissues were blinded to fertility status. (*C*) Immunoblot showing reduction in IQGAP1 protein following HEEC transfection with miR-124-3p mimic (10 nM, N = 4 to 6). (*D* and *E*) HTR8/SVneo spheroid attachment (*D*) to HEECs following *IQGAP1* knockdown (*E*, qPCR) (N = 4). (*F* and *G*) Target site blocker (TSB) was used to confirm the direct interaction between miR-124-3p and *IQGAP1*. (*F*) miR-124-3p and IQGAP1 TSB binding sequences of *IQGAP1* mRNA. (*G*) HEECs were transfected with miR-124-3p mimic (30 nM) in combination with either *IQGAP1* or control TSB (30 nM) and subjected to immunoblotting to determine expression of IQGAP1 (N = 6). (*H*) Protection of *IQGAP1* via TSB in miR-124-3p overexpressed HEECs were able to improve their adhesion to HTR8/SVneo spheroids (N = 6). (*I*) *Iqgap1* expression in mouse E4 luminal epithelium (intrauterine injection model). Data are presented as mean ± SEM. **P* < 0.05, ***P* < 0.01, ****P* < 0.001.

relatively high level of endogenous miR-124-3p at E3 wildtype mouse luminal epithelium which is likely a mechanism to prevent early attachment. By contrast, miR-124-3p was reduced at E4 wildtype mouse uterine luminal epithelium during the receptive window. This timing is similar to human endometrium where we demonstrated that miR-124-3p expression was low in the luminal epithelium during the receptive phase in women with normal fertility but abnormally increased in women with primary infertility. Our data suggested miR-124-3p needed to be downregulated in the endometrial epithelium to enable embryo attachment, likely by increasing factors required for endometrial receptivity in both humans and mice. We confirmed this using a customized array that identified the reduction of many adhesion related genes after miR-124-3p overexpression in both humans and mice. Of note, a spike in expression of certain long noncoding RNAs has been recorded during the receptive window in mice and humans (43, 44). Long noncoding RNAs can function as decoys to bind miRs to prevent their binding to target mRNAs essential for the transition of receptivity (45). For example, long noncoding RNA NEAT1 targets miR-124-3p (46) and its expression is significantly increased in the receptive phase human endometrium (44). Progesterone has also been shown to regulate miR expression (47) and conversely the local expression of miRs can attenuate progesterone signaling to prevent endometrial receptivity (48). It will be of interest in future studies to determine whether miR-124-3p expression changes are related to specific local noncoding RNAs and whether estrogen and progesterone directly or indirectly regulate its levels.

Very few studies have reported culturing human embryos for extended periods to investigate the effects on trophectoderm attachment and development. The available studies have mostly cultured human embryos on the cell culture plates or in Matrigel (49), up to day 11 to 12 postfertilization, the current legal limit (50, 51). It is known that embryos intimately interact and communicate with endometrial epithelial cells where they appose and adhere, prior to implanting (52). It is therefore highly likely that endometrial cells will influence how embryos attach and progress. While human embryos may have the ability to attach to culture wells and develop, development may be different when endometrial cells are present. Here, we cultured primary human trophectoderm spheroids on top of a primary human endometrial 3D bilayer treated with estrogen and progesterone. We altered the levels of miR-124-3p specifically in the endometrial epithelial cells to investigate how the endometrial cell changes influence early trophectoderm attachment and outgrowth in vitro. Our data overall demonstrated that overexpression of miR-124-3p specifically in the HEECs led to reduced firm attachment of the trophectoderm spheroid blocking its development before 120 h of culture (equivalent to day 11 postfertilization). This suggests that in vivo, high levels of miR-124-3p in endometrial epithelium leads to implantation failure and resorption of embryos. These observations concur with the role of miR-124-3p in cancer studies in which it functions as a tumor suppressor inhibiting cell migration and invasion (53). In comparison with previous studies where embryos are cultured on plastic dishes or in Matrigel (49, 51), our data suggested that the trophectoderm grew faster and expanded more rapidly in our coculture model. This remains to be confirmed by comparing embryos cultured on plastic, Matrigel, and endometrial cells in a single experiment. However, our data suggest that while embryos can develop in vitro without endometrial cellular compartments, their growth and development may not accurately reflect what occurs in utero in women. In our current study, we were unable to utilize human embryos with an intact inner cell mass. However, existing data on anembryonic pregnancies suggest that blastocysts without an inner cell mass are capable of attaching and implanting into the endometrium (54). However it remains unknown whether the attachment and early trophoblast development resemble those of intact embryos with an inner cell mass (55). In future studies it will be important to determine whether there are differences in trophectoderm adhesion between intact embryos to endometrial cells with elevated levels of miR-124-3p.

miR-124-3p downregulated *IQGAP1* in both human and mouse endometrial epithelium. IQGAP1 is a scaffold protein that belongs to IQGAP family with three members. While IQGAP2 and -3 have restricted localizations, IQGAP1 is more ubiquitously expressed throughout the body (56). IQGAP1 negatively

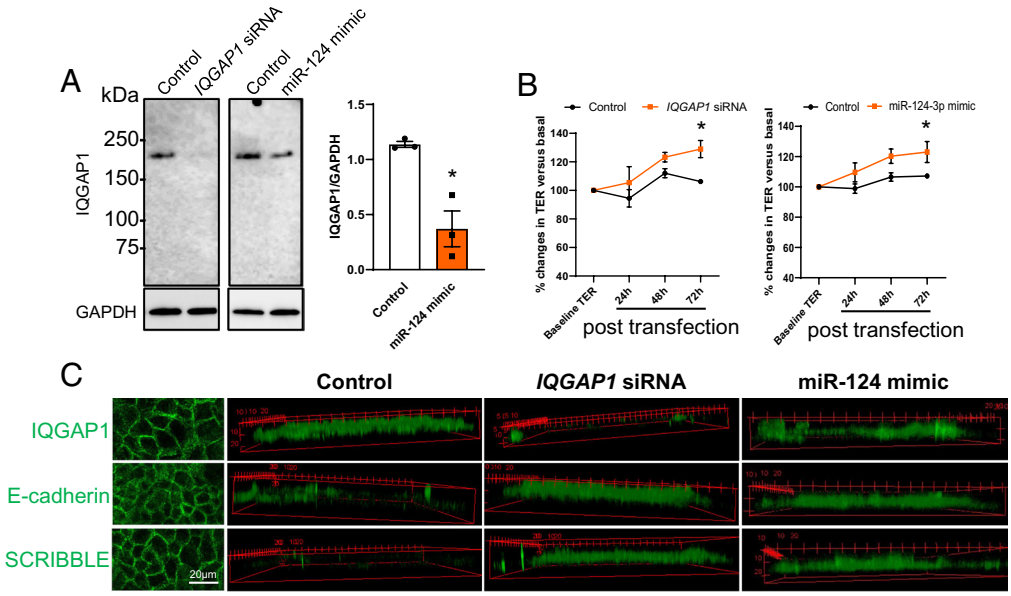

Fig. 8. miR-124-3p overexpression and *IQGAP1* knockdown increased endometrial epithelial cell polarity. (*A*) Immunoblotting identified reduction of IQGAP1 in Ishikawa cells treated with either *IQGAP1* siRNA or miR-124-3p, compared to control. IQGAP1 was undetectable in cells treated with *IQGAP1* siRNA therefore densitometric analysis was not conducted (N = 3). (*B*) To determine cell polarity, Ishikawa cells transfected with *IQGAP1* siRNA, miR-124-3p, or respective controls were subjected to transepithelial electrical resistance assay to monitor percentage changes of cell barrier integrity (N = 5). Data are presented as mean ± SEM. **P* < 0.05. (*C*) 3D lateral scanning of transfected Ishikawa monolayers stained with IQGAP1, E-cadherin, or cell polarity marker SCRIBBLE.

modulates E-cadherin based cell junctions in the human breast epithelial carcinoma cells (57). Here, we further demonstrated that IQGAP1 reduced apical–basal polarity of the endometrial epithelial layer, which is essential to allow embryo attachment (9).

In summary, this study provides strong evidence to support a key role for miR-124-3p in regulating endometrial receptivity by impairing endometrial epithelial cell adhesion and polarity. Targeting miR-124-3p with an inhibitor in HEECs from women with unexplained infertility improved their compromised adhesion, suggesting its potential as a treatment target for endometrial dysfunction. miR-124-3p may also be useful as a biomarker for diagnosing dysregulated receptivity. Patients diagnosed with endometritis have significantly higher serum levels of miR-124-3p when compared to healthy controls (18). Since some women with endometritis may have compromised fertility (58) this suggests that miR-124-3p levels in serum may reflect endometrial physiology. The insights gained from this study could lead to tests to identify women with infertility due to impaired receptivity and interventions to enhance adhesive capacity of endometrial epithelial cells, facilitating embryo adhesion and establishment of pregnancy.

Materials and Methods

Reagents. Antibodies used were summarized in Dataset S3. Primer sequences used were supplied in *SI Appendix*, Table S1. Collagenase was purchased from Worthington (type 3, Lakewood, NJ). miR primers and Transfection reagents (siRNA mimic, miR-124-3p mimic, miR-124-3p inhibitor, Lipofectamine RNAiMAX, Opti-MEM Reduced serum medium) were supplied by Thermo (Waltham, MA). 2′OMe modified and cholesterol conjugated AgomiR-124 and scrambled control were obtained from RiboBio (Guangzhou, China).

Animal Ethics. All experimental procedures involving animals were conducted with the approval of the Animal Ethics Committee at the University of Monash (MMCB/2016/36) and the University of Melbourne (project ID: 10216 and 20395).

Generation and Use of The miR-124-3p Transgenic Mice. Three transgenic mice were crossed to produce the miR-124 mice (*Ltf-iCre*+/−, *CAG-rtTA3*+/−, *Dragon-miR-124-3p*+/−) and control mice (*Ltf-iCre*+/−, *CAG-rtTA3*−/−, *Dragon-miR-124-3p*+/−). The *Ltf-iCre* and *CAG-rtTA3* mice were purchased from the Jackson Laboratory (JAX:026030 and 029627). Dragon-miR-124-3p mice were produced at the Monash Genome Modification Platform.

Determination of miR-124 sequence to be included. Mature miR-124-3p can be transcribed from three different genomic DNA fragments. To determine which fragment to use, we constructed three plasmids, each containing miR124-3p-stem-loop and 200 bp flanking sequence on each side, derived from each of the three genomic fragments (*SI Appendix*, Fig. S1*A*). Using Ishikawa cells and the same doxycycline activation system, we confirmed all three fragments successfully overexpressed mature miR-124-3p in vitro to similar levels (*SI Appendix*, Fig. S1*B*). miR-124-3 was chosen to create the Dragon-miR-124-3p mice. Dragon-miR-124-3 Flp-in vector was built by A.R-D. following the design described in ref. 59, by cloning synthetic miR-124-3 cassette into plasmid pDragon-empty (Addgene #155018). G4 embryonic stem cells (kind gift from Andras Nagy) were modified via homologous recombination, to have a Flp-in landing site at the *Igs7* locus (chr9:21,271,659) using Addgene plasmid #61580 (kind gift from Hongkui Zeng) as targeting vector. Following this, the landing-site embryonic stem cells underwent recombinase-mediated cassette exchange using the Flp-in vector Dragon-miR-124-3. One of the confirmed clones was selected to generate the *Dragon-miR-124-3p* mice. In summary, the *Dragon-miR-124-3p* mouse had a DNA fragment of TRE-Loxp-tdTomato-STOP-Loxp-miR-124-WPRE inserted in an intergenic sequence of chromosome 9 (*SI Appendix*, Fig. S1*A*). WPRE (Woodchuck hepatitis virus Posttranscriptional Regulatory Element) is used to enhance miR-124 expression (*SI Appendix*, Fig. S1*A*).

Confirmation of Dragon system activation in mouse uterine epithelium. Ltf-iCre primarily drives recombination in the uterine epithelium (26) and rtTA3 protein activates the Tet-responsive element in the *Dragon* allele only if bound by doxycycline. Therefore, miR-124 overexpression can be induced specifically in the endometrial epithelium at the desired times by doxycycline administration. Having created the transgenic miR-124-3p mice, we first confirmed the expression of *iCre* and *rtTA3* in the uterus by qPCR (*SI Appendix*, Fig. S1*C*). Transgenic control mouse uterus also expressed *iCre* but not *rtTA3* as *iCre*+/*rtTA3*− genotype was used as a control. None of them were recorded in wildtype mouse uterus (*SI Appendix*, Fig. S1*C*). Using immunofluorescence, we visualized the Ltf-iCre activity in the uterine epithelium by absence of tdTomato fluorescence (*SI Appendix*, Fig. S1*D*). These data also confirmed that the activation of Dragon-miR-124-3p was dependent on rtTA3 because no tdTomato fluorescence was observed in the whole uterus of control mice (*rtTA3*−) after doxycycline administration (*SI Appendix*, Fig. S1 *D*, *Right* panel).

Optimization of doxycycline administration. Doxycycline is required to activate TRE promoter. To rapidly activate the Dragon system, we chose intraperitoneal injection to deliver doxycycline. A time course experiment was first conducted to optimize time of treatment in which a single intraperitoneal injection of doxycycline (80 μg/g body weight) was given to each unpregnant female. Mice were then culled at 4, 12, 24, and 48 h and uteri were collected to examine miR-124-WPRE transcription by qPCR. We recorded a significant increase in *miR-124-WPRE* expression in the luminal epithelium and remaining uterus only at 4 and 12 h compared to control respectively (*SI Appendix*, Fig. S1*E*). Following optimization, plugged miR-124 or control mice were given four injections of doxycycline (80 μg/g body weight) between E2 9 pm and E4 9 am.

Intrauterine Injection. Adult female mice (C57BL6/J) were mated to male mice. Ten μg (in 20 μL saline) AgomiR-124 mimic or scrambled control (2′OMe modified and cholesterol conjugated) were delivered into the uterine horn via intrauterine injection at E3 (Fig. 3*A*). To confirm the successful delivery, mouse uteri were collected at E4 (prior to implantation) and the luminal epithelium was separated from the uterus via Dispase (0.5% in Hank's Balanced Salt Solution) digestion for 2 h at room temperature (RT). The luminal epithelium and remaining uterus were used for qPCR to determine miR-124-3p and target genes expression.

Mouse Embryo Transfection, Hatching, Zona Pellucida Breaking, and Outgrowth. Mouse concepti were collected at E1 and cultured in G1 plus medium for 72 h until concepti reached the morulae stage (when in vivo embryos were exposed to miR-124-3p). E3 embryos were treated with fluorescently labeled miR-124-3p mimic or scrambled control (100 nM) using the lipofectamine RNAiMAX based transfection system (1% lipofectamine in blastocyst culture medium). Embryos were then cultured in G1-plus based transfection medium for 24 h and the uptake of miR-124-3p (visualized by fluorescence) was recorded by confocal microscopy. Unhatched embryos (E4) were treated with the same transfection mixture for 72 h to record the effects on hatching, zona pellucida breaking, and outgrowth using the MIRI time-lapse system (Esco). Successful miR-124-3p overexpression was confirmed by qPCR.

Human Sample Collection and Ethics Statement (Endometrial Tissue and Embryo). Endometrial tissue: Written informed consent was obtained from each patient and the study was approved by the Human Research Ethics Committee at Monash Health and the Royal Women's Hospital (ID: #03066B). All women had regular menstrual cycles, were not using intrauterine contraceptives and had not used hormones for at least 3 mo before surgery. Fertile women had proven parity and infertile women had primary unexplained infertility. The collected endometrium were examined by experienced gynecological pathologists to confirm the cycle stage and absence of apparent endometrial dysfunction such as chronic endometritis and endometriosis. Defective receptivity is a significant factor contributing to the etiology of unexplained infertility (60). Human embryo: The usage of human embryos was approved by the NHMRC Human Embryo Research License (ID: #309722). Embryos (surplus) were created using either conventional IVF or Intracytoplasmic Sperm Injection. The detailed protocol of embryo vitrification, thawing, allotment, and culture was established in our previous study (61) with the modification of removing the inner cell mass due to consent restrictions. The inner cell mass was removed to ensure couples donating excess embryos were comfortable for research to be performed on this material. While the inner cell mass was removed, the embryos were still able to re-expand and we could evaluate embryonic trophectoderm adhesion to the endometrial cocultured cells. To remove inner cell mass, mechanical dissection was performed on fully hatched

embryos using a 35 μm diameter biopsy pipette (TPC, LBC-OD35BA90) on a Transferman micromanipulation system. Resultant trophectoderm were allowed to reform into spheroids (occurred within 2 h) and used immediately.

HEEC and Stromal Cell Isolation and In Vitro Culture Models. Collected endometrium (day 7 to 18 of the menstrual cycle) were subjected to HEEC and stromal cell isolation as previously published (62). The method of HTR8/SVneo spheroid adhesion on HEEC monolayer was detailed described in our previous study (17). The other two models using the 3D endometrial construct were prepared as previously described (63). 3D endometrial constructs were treated with 0.3 nmol/L estrogen and 900 nmol/L progesterone for 1 d before adding primary human trophectoderm spheroids. The attachment and outgrowth of primary human trophectoderm spheroids on endometrial construct was recorded up to 120 h. Firm attachment of the trophectoderm spheroids was determined by gently shaking the culture plates under microscopy.

miR-124-3p Mimic and Inhibitor, Target Site Blocker, and Target Genes siRNA Transfection. Cells were cultured to 70% confluence then transfected with Lipofectamine RNAiMAX and Opti-MEM medium containing miR-124-3p mimic (10 nM), miR-124-3p inhibitor (30 nM), siRNA mimic (10 nM), or scrambled controls. TSB (30 nM) was cotransfected with miR-124-3p mimic (30 nM) to investigate the direct interaction between miR-124-3p and *IQGAP1*. After 24 h the transfection medium was replaced with fresh culture medium and cells were cultured for 48 h before being subjected to spheroid adhesion assay or other analyses.

Transepithelial Electrical Resistance. 2×10^5 Ishikawa cells were seeded on each extracellular matrix (1:10 Matrigel/DMEM) coated trans-well insert (6.5 mm, 0.4 μm pore, Corning). Cells were cultured in DMEM containing 10% fetal bovine serum overnight to allow attachment and then switched to 0.5% fetal bovine serum. After 24 h of culturing, the Millipore MilliCell-Electrical Resistance System (Millipore) was used to measure the baseline electrical resistance. Cells were then transfected as described above. Following transfection, cells were maintained under DMEM containing 0.5% fetal bovine serum, and transepithelial electrical resistance was measured daily for three days. Changes in transepithelial electrical resistance were determined relative to the baseline readings, expressed as a percentage for each condition.

RNA Isolation, RT-qPCR, and Customized PCR Array. Total RNA was isolated using the TriReagent or RNeasy Mini Kit (Qiagen) or RNeasy Micro Kit (Qiagen, for mouse embryos). miR-124-3p PCR was conducted using the Taqman miR reverse transcription kit and Universal Master Mix II according to the manufacturer's instructions (Thermo). For gene targets detection, 300 ng total RNA was converted to cDNA using SuperScript™ III First-Strand Synthesis System. miR-124-3p expression was normalized to U44 (human) or U6 (mouse). Gene expression was normalized to *18S*. Relative expression levels were calculated using the comparative cycle threshold method (ΔΔCt). Customized PCR array was conducted according to the manufacturer's instructions (Qiagen). miRWalk was used to select putative miR-124-3p targets.

Immunohistochemistry and Immunofluorescence. Tissues were fixed in 10% formalin, embedded in paraffin and sectioned at 4 μm thickness. Slides were dewaxed, rehydrated, and subjected to antigen retrieval as summarized in Dataset S3. Endogenous peroxidase was blocked using 3% hydrogen peroxide in methanol for 15 min. Nonimmune blocking was completed with 10% goat serum and 2% human serum (human tissue) or 2% mouse serum (mouse tissue) in Tris-buffered saline (TBS) for 1 h at RT. Slides were then incubated with primary antibodies at 4 °C overnight (dilution of all antibodies in Dataset S3). An isotype control was included in which sections were incubated with nonimmune antibody of the same isotype as the primary antibody at the same concertation. Positive signal was visualized via Diaminobenzidine. Staining intensity scores were determined by two individual scorers blinded to the patient characteristic.

For immunofluorescent staining, cultured cells were fixed with 4% paraformaldehyde for 15 min. Cells were blocked in 3% bovine serum albumin (BSA)/Phosphate-buffered saline (PBS) at RT for 1 h and subjected to overnight incubation of primary antibodies at 4 °C. After washing with PBS, cells were incubated with Alexa Fluor 488-conjugated antisera at RT for 1 h. 3D lateral labeling of IQGAP1, E-cadherin, and SCRIBBLE was scanned using Z-stack confocal imaging.

In Situ Hybridization. MiRCURY LNA miRNA ISH Optimization kit was used with the detailed protocol provided by Qiagen. The following conditions were optimized from previously published protocols (64) for human miR-124-3p probe: Proteinase K incubation was performed at 37 °C for 10 min. hsa-miR-124-3p custom detection probe (100 nM), hsa-LNA U6 snRNA positive control probe (80 nM), hsa-LNA scrambled control probe (100 nM) hybridization was performed for 60 min at 60 °C. For mouse in situ hybridization, mmu-miR-124-3p detection probe (#339115, Qiagen) and mmu-miR-scramble control probe (#339111, Qiagen) were incubated at 55 °C at a concentration of 50 nM. Sections were then blocked with 10% CAS block (Invitrogen), 2% sheep serum, and 1% BSA in PBST (0.1% Tween) for 15 min (human sections) or 30 min (mouse sections) at RT. Fluorescent anti-DIG reagent was diluted 1:50 (human sections) or 1:200 (mouse sections) in a diluent solution containing PBS and 1% sheep serum and BSA and incubated on sections for 1 h at RT. Sections were counterstained with DAPI to indicate the nuclei.

Immunoblotting. Cells were lysed in ice-cold lysis buffer (50 mM Tris·HCl [pH 7.5], 150 mM NaCl, 2 mM EDTA, 2 mM EGTA, 25 mM NaF, 25 mM β-glycerolphosphate, protease inhibitor mixture). Proteins were resolved by SDS-PAGE (150 V, 1 h) and transferred to PVDF membranes (100 V, 1 h). Membranes were blocked with 5% skim milk and incubated with antibodies as summarized in Dataset S3. After overnight incubation at 4 °C, membranes were washed with TBS-Tween 0.1% (v/v) and incubated with HRP conjugated secondary antibodies. Labeled proteins were detected by chemiluminescence (Thermo). Membranes were stripped and incubated with anti-GAPDH as a loading control. Protein band intensity was determined using ImageJ.

hCG ELISA. Human hCG ELISA kit was purchased from Thermo (EHCG) with a sensitivity of 50 pg/mL. ELISA was conducted according to the manufacturer's instructions. Pregnant human serum was diluted 1:4 and used as a positive control. Absorbance was measured at 450 nm. A concentration of 46,127 pg/mL hCG was detected in diluted pregnant human serum (7,500 pg/mL equals 22.5 mIU/L).

Statistical Analysis. Experiments reported in this study were repeated on at least three biological samples (indicated in figure legends). Statistical analysis was carried out using PRISM 8.0 and student's *t* test or one-way ANOVA as appropriate. $P < 0.05$ was considered statistically significant.

Data, Materials, and Software Availability. All study data are included in the article and/or supporting information.

ACKNOWLEDGMENTS. We are grateful to Ms Judi Hocking and Ms Emily-jane Bromley for orchestrating the tissue collection and the women who donated the endometrial tissue and embryos. We are also grateful to Dr. Meaghan Griffiths (Monash University) for technical assistance, Dr. Jeremy Cottrell (University of Melbourne) for the assistance of transepithelial electrical resistance assay and Biological Optical Microscopy Platform (University of Melbourne) for the assistance of confocal imaging. We thank Single Cell and High Throughput Genomics Centre based at The Hudson Institute of Medical Research for the assistance of Fluidigm BioMark HD analysis. This work was supported by a National Health and Medical Research Council of Australia Project Grant (APP1120689) to E.D. and L.R. and a senior research fellowship to E.D. (#550905). W.Z. was supported by an Early Career Researcher Grant, Department of Obstetrics and Gynaecology fellowship and the Rowden White Trust Foundation (University of Melbourne).

Author affiliations: [a]Department of Obstetrics, Gynaecology and Newborn Health, University of Melbourne, Parkville, VIC 3010, Australia; [b]Gynaecology Research Centre, Royal Women's Hospital, Parkville, VIC 3052, Australia; [c]Centre for Reproductive Health, The Hudson Institute of Medical Research, Clayton, VIC 3168, Australia; [d]Department of Anatomy and Developmental Biology, University of Monash, Clayton, VIC 3800, Australia; [e]Department of Obstetrics and Gynaecology, University of Monash, Clayton, Victoria 3800, Australia; [f]Faculty of Animal Husbandry, Jenderal Soedirman University, Purwokerto 53122, Indonesia; [g]Monash In Vitro Fertilisation, Clayton, VIC 3168, Australia; [h]Australian Regenerative Medicine Institute, Monash University, Clayton, VIC 3800, Australia; [i]Department of Physiology, Development and Neuroscience, The Centre for Trophoblast Research, University of Cambridge, Cambridge CB2 3EL, United Kingdom; and [j]Department of Genetics, University of Cambridge, Cambridge CB2 3EH, United Kingdom

Author contributions: W.Z., M.V.S., M.P., A.R.-D., and E.D. designed research; W.Z., M.V.S., K.R., E.M., K.S., M.P., and L.S. performed research; K.S., T.O., L.R., and A.R.-D. contributed new reagents/analytic tools; W.Z., M.V.S., L.S., and E.D. analyzed data; T.O. and L.R. collected the human blastocyst trophectoderm; and W.Z., E.M., and E.D. wrote the paper.

1. A. J. Wilcox, D. D. Baird, C. R. Weinberg, Time of implantation of the conceptus and loss of pregnancy. *N. Engl. J. Med.* **340**, 1796–1799 (1999).
2. L. Kao *et al.*, Global gene profiling in human endometrium during the window of implantation. *Endocrinology* **143**, 2119–2138 (2002).
3. T. Strowitzki, A. Germeyer, R. Popovici, M. Von Wolff, The human endometrium as a fertility-determining factor. *Hum. Reprod. Update* **12**, 617–630 (2006).
4. A. Psychoyos, Uterine receptivity for nidation. *Ann. N. Y. Acad. Sci.* **476**, 36–42 (1986).
5. B. Paria, Y. Huet-Hudson, S. Dey, Blastocyst's state of activity determines the "window" of implantation in the receptive mouse uterus. *Proc. Natl. Acad. Sci. U.S.A.* **90**, 10159–10162 (1993).
6. A. PSychoyos, Endocrine control of egg implantation. *Handb. Physiol.* **2**, 187–215 (1973).
7. S. Whitby, W. Zhou, E. Dimitriadis, Alterations in epithelial cell polarity during endometrial receptivity: A systematic review. *Front. Endocrinol.* **11**, 596324 (2020).
8. M. Thie *et al.*, Cell adhesion to the apical pole of epithelium: A function of cell polarity. *Eur. J. Cell Biol.* **66**, 180–191 (1995).
9. T. Daikoku *et al.*, Conditional deletion of Msx homeobox genes in the uterus inhibits blastocyst implantation by altering uterine receptivity. *Dev. Cell* **21**, 1014–1025 (2011).
10. D. Martel, M. Monier, D. Roche, A. Psychoyos, Hormonal dependence of pinopode formation at the uterine luminal surface. *Hum. Reprod.* **6**, 597–603 (1991).
11. S. Heng *et al.*, Podocalyxin inhibits human embryo implantation in vitro and luminal podocalyxin in putative receptive endometrium is associated with implantation failure in fertility treatment. *Fertil. Steril.* **116**, 1391–1401 (2021).
12. C. Shi *et al.*, Endometrial microRNA signature during the window of implantation changed in patients with repeated implantation failure. *Chin. Med. J. (Engl.)* **130**, 566 (2017).
13. A. Riyanti *et al.*, Suppressing HOXA-10 gene expression by microRNA 135b during the window of implantation in infertile women. *J. Reprod. Infertil.* **21**, 217 (2020).
14. K. Rekker *et al.*, A two-cohort RNA-seq study reveals changes in endometrial and blood miRNome in fertile and infertile women. *Genes* **9**, 574 (2018).
15. J. O'Brien, H. Hayder, Y. Zayed, C. Peng, Overview of microRNA biogenesis, mechanisms of actions, and circulation. *Front. Endocrinol. (Lausanne)* **9**, 402 (2018).
16. V. A. Gennarino *et al.*, HOCTAR database: A unique resource for microRNA target prediction. *Genes* **480**, 51–58 (2011).
17. M. Griffiths, M. Van Sinderen, K. Rainczuk, E. Dimitriadis, miR-29c overexpression and COL4A1 downregulation in infertile human endometrium reduces endometrial epithelial cell adhesive capacity in vitro implying roles in receptivity. *Sci. Rep.* **9**, 8644 (2019).
18. C. Di Pietro *et al.*, MiR-27a-3p and miR-124-3p, upregulated in endometrium and serum from women affected by Chronic Endometritis, are new potential molecular markers of endometrial receptivity. *Am. J. Reprod. Immunol.* **80**, e12858 (2018).
19. C. A. White *et al.*, Blocking LIF action in the uterus by using a PEGylated antagonist prevents implantation: A nonhormonal contraceptive strategy. *Proc. Natl. Acad. Sci. U.S.A.* **104**, 19357–19362 (2007).
20. S. Pawar *et al.*, STAT3 regulates uterine epithelial remodeling and epithelial-stromal crosstalk during implantation. *Mol. Endocrinol.* **27**, 1996–2012 (2013).
21. C. L. Stewart *et al.*, Blastocyst implantation depends on maternal expression of leukaemia inhibitory factor. *Nature* **359**, 76–79 (1992).
22. A. Majid *et al.*, miR-124-3p suppresses the invasiveness and metastasis of hepatocarcinoma cells via targeting CRKL. *Front. Mol. Biosci.* **7**, 223 (2020).
23. L. Deng *et al.*, Bioengineered miR-124-3p prodrug selectively alters the proteome of human carcinoma cells to control multiple cellular components and lung metastasis in vivo. *Acta Pharm. Sin. B* **11**, 3950–3965 (2021).
24. S. Altmäe *et al.*, Endometrial gene expression analysis at the time of embryo implantation in women with unexplained infertility. *Mol. Hum. Reprod.* **16**, 178–187 (2009).
25. A. Roselló-Díez, L. Madisen, S. Bastide, H. Zeng, A. L. Joyner, Cell-nonautonomous local and systemic responses to cell arrest enable long-bone catch-up growth in developing mice. *PLoS Biol.* **16**, e2005086 (2018).
26. T. Daikoku *et al.*, Lactoferrin-iCre: A new mouse line to study uterine epithelial gene function. *Endocrinology* **155**, 2718–2724 (2014).
27. L. E. Dow *et al.*, Conditional reverse tet-transactivator mouse strains for the efficient induction of TRE-regulated transgenes in mice. *PLoS ONE* **9**, e95236 (2014).
28. W. Zhou, E. Menkhorst, E. Dimitriadis, Jagged1 regulates endometrial receptivity in both humans and mice. *FASEB J.* **35**, e21784 (2021).
29. Y. S. Kim *et al.*, An unanticipated discourse of HB-EGF with VANGL2 signaling during embryo implantation. *Proc. Natl. Acad. Sci. U.S.A.* **120**, e2302937120 (2023).
30. H. Lim *et al.*, Multiple female reproductive failures in cyclooxygenase 2–deficient mice. *Cell* **91**, 197–208 (1997).
31. K. Y. Lee *et al.*, Bmp2 is critical for the murine uterine decidual response. *Mol. Cell Biol.* **27**, 5468–5478 (2007).
32. Q. Li *et al.*, The antiproliferative action of progesterone in uterine epithelium is mediated by Hand2. *Science* **331**, 912–916 (2011).
33. H. L. Franco *et al.*, WNT4 is a key regulator of normal postnatal uterine development and progesterone signaling during embryo implantation and decidualization in the mouse. *FASEB J.* **25**, 1176 (2011).
34. N. A. Rashid, S. Lalitkumar, P. G. Lalitkumar, K. Gemzell-Danielsson, Endometrial receptivity and human embryo implantation. *Am. J. Reprod. Immunol.* **66**, 23–30 (2011).
35. P. Vergaro, G. Tiscornía, A. Rodriguez, J. Santaló, R. Vassena, Transcriptomic analysis of the interaction of choriocarcinoma spheroids with receptive vs. non-receptive endometrial epithelium cell lines an in vitro model for human implantation. *J. Assist. Reprod. Genet.* **36**, 857–873 (2019).
36. D. E. Levy, C.-K. Lee, What does Stat3 do? *J. Clin. Invest.* **109**, 1143–1148 (2002).
37. E. B. Samson *et al.*, The coordinating role of IQGAP1 in the regulation of local, endosome-specific actin networks. *Biol. Open* **6**, 785–799 (2017).
38. S. Whitby, L. A. Salamonsen, J. Evans, The endometrial polarity paradox: Differential regulation of polarity within secretory-phase human endometrium. *Endocrinology* **159**, 506–518 (2018).
39. B. Paria, H. Lim, S. Das, J. Reese, S. Dey, Molecular signaling in uterine receptivity for implantation. *Semin. Cell Dev. Biol.* **11**, 67–76 (2000).
40. L.-J. Shen *et al.*, Mmu-microRNA-200a overexpression leads to implantation defect by targeting phosphatase and tensin homolog in mouse uterus. *Reprod. Sci.* **20**, 1518–1528 (2013).
41. K. Yoshinaga, A sequence of events in the uterus prior to implantation in the mouse. *J. Assist. Reprod. Genet.* **30**, 1017–1022 (2013).
42. D. Flores, M. Madhavan, S. Wright, R. Arora, Mechanical and signaling mechanisms that guide pre-implantation embryo movement. *Development* **147**, dev193490 (2020).
43. Q. Wang *et al.*, Genome-wide analysis and functional prediction of long non-coding RNAs in mouse uterus during the implantation window. *Oncotarget* **8**, 84360 (2017).
44. B. Sigurgeirsson *et al.*, Comprehensive RNA sequencing of healthy human endometrium at two time points of the menstrual cycle. *Biol. Reprod.* **96**, 24–33 (2017).
45. M. Takamura, W. Zhou, L. Rombauts, E. Dimitriadis, The long noncoding RNA PTENP1 regulates human endometrial epithelial adhesive capacity in vitro: Implications in infertility. *Biol. Reprod.* **102**, 53–62 (2019).
46. D. Yuan *et al.*, Expression of lncRNA NEAT1 in endometriosis and its biological functions in ectopic endometrial cells as mediated via miR-124-3p. *Genes Genomics* **44**, 527–537 (2022).
47. Y. Hirota, "Uterine receptivity in mouse embryo implantation" in *Uterine Endometrial Function*, H. Kanzaki, Ed. (Springer, 2016), pp. 11–25.
48. H. Haraguchi *et al.*, MicroRNA-200a locally attenuates progesterone signaling in the cervix, preventing embryo implantation. *Mol. Endocrinol.* **28**, 1108–1117 (2014).
49. L. Xiang *et al.*, A developmental landscape of 3D-cultured human pre-gastrulation embryos. *Nature* **577**, 537–542 (2020).
50. A. Deglincerti *et al.*, Self-organization of the in vitro attached human embryo. *Nature* **533**, 251–254 (2016).
51. M. N. Shahbazi *et al.*, Self-organization of the human embryo in the absence of maternal tissues. *Nat. Cell Biol.* **18**, 700–708 (2016).
52. S. Shibata *et al.*, Modeling embryo-endometrial interface recapitulating human embryo implantation. *Sci. Adv.* **10**, eadi4819 (2024).
53. J.-R. Wang, B. Liu, L. Zhou, Y.-X. Huang, MicroRNA-124-3p suppresses cell migration and invasion by targeting ITGA3 signaling in bladder cancer. *Cancer Biomark.* **24**, 159–172 (2019).
54. F.-T. Kung, Hysteroscopic differences in the gestational sac in asymptomatic blighted ovum and viable pregnancy at early gestation. *Taiwanese J. Obstet. Gynecol.* **44**, 342–346 (2005).
55. F. Albayram, U. M. Hamper, First-Trimester obstetric emergencies: Spectrum of sonographic findings. *J. Clin. Ultrasound* **30**, 161–177 (2002).
56. M. D. Brown, D. B. Sacks, IQGAP1 in cellular signaling: Bridging the GAP. *Trends Cell Biol.* **16**, 242–249 (2006).
57. Z. Li, S. H. Kim, J. M. Higgins, M. B. Brenner, D. B. Sacks, IQGAP1 and calmodulin modulate E-cadherin function. *J. Biol. Chem.* **274**, 37885–37892 (1999).
58. H. J. Park, Y. S. Kim, T. K. Yoon, W. S. Lee, Chronic endometritis and infertility. *Clin. Exp. Reprod. Med.* **43**, 185 (2016).
59. E. Ahmadzadeh *et al.*, A collection of genetic mouse lines and related tools for inducible and reversible intersectional mis-expression. *Development* **147**, dev186650 (2020).
60. B. Bui *et al.*, Does endometrial scratching increase the rate of spontaneous conception in couples with unexplained infertility and a good prognosis (Hunault> 30%)? Study protocol of the SCRaTCH-OFO trial: A randomized controlled trial. *BMC Pregnancy Childbirth* **18**, 1–9 (2018).
61. S. Lalitkumar *et al.*, Polyethylene glycated leukemia inhibitory factor antagonist inhibits human blastocyst implantation and triggers apoptosis by down-regulating embryonic AKT. *Fertil. Steril.* **100**, 1160–1169 (2013).
62. E. Dimitriadis, L. Robb, L. Salamonsen, Interleukin 11 advances progesterone–induced decidualization of human endometrial stromal cells. *Mol. Hum. Reprod.* **8**, 636–643 (2002).
63. P. Lalitkumar *et al.*, Mifepristone, but not levonorgestrel, inhibits human blastocyst attachment to an in vitro endometrial three-dimensional cell culture model. *Hum. Reprod.* **22**, 3031–3037 (2007).
64. S. Barton *et al.*, miR-23b-3p regulates human endometrial epithelial cell adhesion implying a role in implantation. *Reproduction* **165**, 407–416 (2023).